Since January 2020 Elsevier has created a COVID-19 resource centre with free information in English and Mandarin on the novel coronavirus COVID-19. The COVID-19 resource centre is hosted on Elsevier Connect, the company's public news and information website.

Journal of Controlled Release 275 (2018) 53–66

Contents lists available at ScienceDirect

Journal of Controlled Release

journal homepage: www.elsevier.com/locate/jconrel

Macromolecular prodrugs of ribavirin: Polymer backbone defines blood safety, drug release, and efficacy of anti-inflammatory effects

Kaja Zuwala[a,b,1], Camilla F. Riber[b,1], Kaja Borup Løvschall[b], Anna H.F. Andersen[a,b], Lise Sørensen[b], Paulina Gajda[a], Martin Tolstrup[a], Alexander N. Zelikin[b,c,*]

[a] Department of Infectious Diseases, Aarhus University Hospital, 8200, Denmark
[b] Department of Chemistry, Aarhus University, 8000, Denmark
[c] iNano Interdisciplinary Nanoscience Centre, Aarhus University, 8000, Denmark

ARTICLE INFO

Keywords:
Antiviral
Macrmolecular prodrug
Albumin
Drug release

ABSTRACT

Macromolecular (pro)drugs hold much promise as broad-spectrum antiviral agents as either microbicides or carriers for intracellular delivery of antiviral drugs. Intriguing opportunity exists in combining the two modes of antiviral activity in the same polymer structure such that the same polymer acts as a microbicide and also serves to deliver the conjugated drug (ribavirin) into the cells. We explore this opportunity in detail and focus on the polymer backbone as a decisive constituent of such formulations. Fourteen polyanions (polycarboxylates, polyphosphates and polyphosphonates, and polysulfonates) were analyzed for blood pro/anti coagulation effects, albumin binding and albumin aggregation, inhibitory activity on polymerases, cytotoxicity, and anti-inflammatory activity in stimulated macrophages. Ribavirin containing monomers were designed to accommodate the synthesis of macromolecular prodrugs with disulfide-exchange triggered drug release. Kinetics of drug release was fast in all cases however enhanced hydrophobicity of the polymer significantly slowed release of ribavirin. Results of this study present a comprehensive view on polyanions as backbone for macromolecular prodrugs of ribavirin as broad-spectrum antiviral agents.

1. Introduction

Viruses are fascinating products of evolution and life-threatening pathogens at the same time. Indeed, these non-cellular assemblies of macromolecules and lipids are simpler than even minimalistic replicating cells but can infect living organisms in both plant and animal kingdoms. Throughout history, viral infections repeatedly had a devastating effect on human society and even in modern times, viral outbreaks create an enormous socio-economic burden [1,2]. Recent examples include the outbreaks of coronavirus-associated Southeast Asian and Middle Eastern Respiratory Syndromes (SARS, MERS) as well as the Ebola and Zika virus outbreaks. To counter this, interdisciplinary efforts have been made over the past decades in the design and development of antiviral drugs. In large part, this was spurred by the spread of the human immunodeficiency virus (HIV) [3]. Currently, there are nearly one hundred antiviral drugs approved by the US FDA [4]. Nevertheless, significant challenges remain. It is now understood that a significant limitation of current strategies is that countermeasures to viral pathogens are most typically developed individually and specifically to each emerging pathogen. An aspect that came into the focus of research attention is the development of “broad-spectrum antiviral agents” [5].

Such agents can constitute prophylactic, [6] preventative, [7,8] or curative [9,10] measures. Prophylaxis (vaccination) holds a great appeal but universal antiviral vaccines are yet to be developed [6]. In fact, the overall majority of pathogenic viruses have no corresponding vaccination product. In turn, curative measures are highly attractive in their own right. However, while replicational cycles of viruses are similar, there is a great variability between viral enzymes and other proteins that could serve as drug targets – making the design of universal antiviral agents challenging [4]. Interferon is an endogenous protein that serves as a potent stimulatory signal to human immunity and acts as a non-specific, broadly acting antiviral agent. However, viruses developed multiple interferon inhibitors which compromise induction or activity of interferon [11]. Moreover, due to its side effects, its clinical use is limited [12]. Several small molecule drugs also serve as broadly acting antivirals. Of these, ribavirin (RBV) has a long history of medicinal use and appears on the World Health Organization

* Corresponding author.
E-mail address: zelikin@chem.au.dk (A.N. Zelikin).
[1] Contributed equally.

https://doi.org/10.1016/j.jconrel.2018.02.012
Received 27 October 2017; Received in revised form 2 February 2018; Accepted 8 February 2018
Available online 09 February 2018
0168-3659/

list of essential medicines for both adults and children [13,14]. However, this drug also has a dose limiting toxicity. Several other experimental drug leads are in different stages of (pre)clinical development [15–18].

Finally, preventative antivirals that act through neutralization of viruses and/or blocking virus cell entry appear to be highly promising as broad-spectrum antiviral agents [19–21]. A notable class of such agents is polymers. In the early 1940s, it was first observed that viruses interact with polymers [22] and inhibit virus infectivity [23]. Over subsequent decades, this effect was shown to be affecting viral pathogens across the viral genus and families, and observed for polymers diverse in their structure, natural and synthetic, positively or negatively charged [24–29]. De Clercq et al. proposed that activity of the negatively charged polymers, at least in vivo, is indirect and proceeds via stimulation of interferon production [30]. However, antiviral activity proceeds potently and efficaciously in vitro, in absence of interferon, and the direct contact between polymers and the virus with ensuing neutralizing activity is now well-documented. Inherent skepticism towards polyanions and other polymers as antivirals [31] originates in the failures of hallmark clinical trials for these agents both when administered systemically or as topical microbicides [7]. Specifically for systemic administration, it has been concluded that preventative antiviral effect would have to rely on a sustained, high concentration of these agents in blood not achievable without toxic effects [31]. However, other polymers are successfully commercialized as antivirals, specifically as lubricants in condoms acting as microbicides with activity against HIV and herpes simplex viruses [32]. Nucleic acid based polyanions progress through clinical trials as agents against hepatitis B virus with potential of further development as broad-spectrum antiviral activity [20]. It is important to note that failed clinical trials are indeed discouraging yet important, game-changing developments have occurred in polymer chemistry in recent decades. Specifically, novel polymerization techniques are now available to afford polymers with well-controlled molar mass and architecture and a significantly broader available polymer functionality (side chains) [33,34]. Another notable advancement includes the development of polymeric virucidal agents that compromise stability of the viral envelope and exert permanent damage to the virion [35,36]. Together, the broad spectrum of activity of polymers against viral pathogens and the chemical versatility of these agents renders this class of antiviral agents unique and attractive for deeper investigation.

In our past studies, we developed broad-spectrum antiviral agents based on macromolecular prodrugs (MP) of ribavirin. When conjugated to polymers, ribavirin did not accumulate in the red blood cells which in vivo is the main side effect of the drug [37–39]. MP of ribavirin broadened the therapeutic window of the drug (in vitro) [37] and were effective against diverse viruses such as HCV (in a replicon cell culture model), measles, and influenza, in the latter case revealing antiviral effects in chicken embryo model [40,41]. We also experimentally confirmed the link between ribavirin and the synthesis of nitric oxide in macrophages, with relevance to the treatment of hepatitis [42]. Key to successful delivery of ribavirin using MP was the development of a disulfide-containing linker that releases the drug from the prodrug upon cell entry [43].

From a different perspective, we also focused on preventative measures and conducted a systematic study of polymers with anionic charge as inhibitors of virus cell entry [21]. Our broad study considered 14 polymers, infectious Zika virus, HIV, and HSV, as well as pseudotyped viral particles for Ebola, Lassa, Lyssa, SARS, and other viruses. The main finding of our work was that anionic charge alone (be it carboxylate, phosphate/phosphonate, or sulfonate) did not endow the polymer with broad-spectrum antiviral activity. Decisive factor for such activity was the enhanced (but balanced) hydrophobicity of the macromolecule. Identified lead candidate polymers exhibited antiviral activity against all the enveloped viral pathogens, including the Zika virus. For the latter, we presented evidence of direct contact between the polymer and the viral particle and concurrent inhibition of viral infectivity [21].

One intriguing possibility lies in the prospect of combining the curative and the preventative antiviral activity within the same macromolecular antiviral agent [40,44]. Such agents represent a combination therapy wherein the carrier exerts extracellular preventative effect [21] whereas the conjugated drug, once released inside the cell, is an intracellularly active therapeutic [37]. It is also possible that polyanions have an intracellular antiviral effect of their own, that is the inhibition of viral polymerases, [40,45,46] presumably through competitive electrostatic interaction with the protein. In this work, we explore the design of such combination therapy in detail. We focus on the choice of the macromolecular backbone as a carrier for the conjugated drug and analyze blood coagulation, binding to albumin, albumin aggregation, inhibitory activity on polymerases, and cytotoxicity for polymers differed by their anionic charge (carboxylates, phosphates and phosphonates, sulfonates). Further, we synthesize ribavirin-containing counterparts to the polyanions, investigate kinetics of drug release for the resulting macromolecular prodrugs, and investigate their use for intracellular drug delivery of ribavirin in an anti-inflammatory model in macrophages. As a result, we identify polymers and macromolecular prodrugs that are devoid of blood anti-coagulation activity but are strong as inhibitors of polymerases and efficacious as delivery vehicles for ribavirin – thus being attractive for the development of broad-spectrum antiviral agents. We also identified polymers that are benign and devoid of any activity in these tests thus being attractive as "stealth" materials for diverse biomedical applications [47]. Results of this study would be important for the advancement of biomedical engineering, specifically with regards to development of antiviral therapies and drug delivery techniques.

2. Results and discussion

2.1. Polymer synthesis

Homopolymers of 14 different anionic monomers with variations in the anionic functionality (carboxylic acid, sulfonic acid, phosphonic acid and phosphate, Fig. 1) were obtained through the Reversible Addition-Fragmentation chain Transfer (RAFT) polymerization [21]. Synthetic approach to the synthesis of the corresponding macromolecular prodrugs was chosen to proceed via copolymerization of the drug containing monomer and that corresponding to the carrier polymer. Towards this end, RBV containing monomers were designed to be compatible with polymerization of diverse co-monomers, acrylic and methacrylic, hydrophilic and hydrophobic (Fig. 2). Of these, the synthesis of the hydrophobic methacrylate monomer (monomer 1 in Fig. 2) was reported in our previous publications [43]. Acrylic counterparts were obtained via similar protocols with minor variations. Design consideration also concerned polarity of co-monomers, an aspect that exerts limitations to the choice of the solvent for polymerization. Polarity of the applied anionic monomers varied from those with a hydrophilic character (phosphates/phosphonates) to those with well pronounced hydrophobic character (ethylacrylic acid, propylacrylic acid). RBV monomers were therefore designed to mimic the polarity of the anionic comonomers through the use of silyl protecting groups to render the monomer more hydrophobic or using deprotected, hydrophilic 2′,3′-hydroxyl containing monomers. In total four different RBV prodrug monomers were applied (Fig. 2), allowing for the copolymerization to be performed under hydrophobic and hydrophilic conditions with either acrylate/acrylamide or methacrylate/methacrylamide containing monomers. In each case, the monomer structure also comprised a disulfide bond for intracellular degradation, coupled to a self-immolative linker for drug release [48].

Due to the variations in monomer type and monomer polarity, a unique set of reaction conditions was necessary for each copolymerization including the choice of RAFT agent, solvent (or solvent

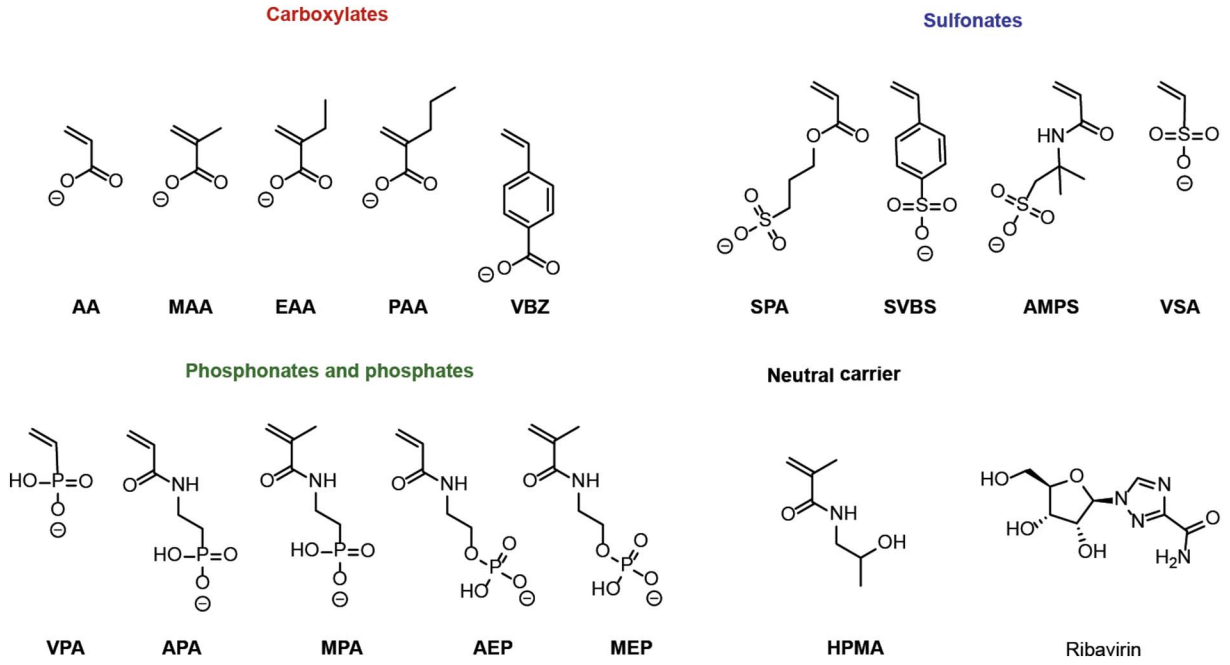

Fig. 1. Anionic monomers (carboxylates, phosphates and phosphonates, and sulfonates) and ribavirin used in this study for the synthesis of polyanions and macromolecular prodrugs as broad-spectrum antiviral agents. Macromolecular prodrugs were synthesized for (meth)acrylates and (meth)acrylamides only (not for VBZ, SVBS, VSA, VPA).

mixture), reaction time, initiator, and purification procedure (Table 1, for full details see Experimental section). Synthesized macromolecular (pro)drugs were analyzed by ^{1}H NMR during synthesis to assess the conversion of the two monomers and in the purified form to confirm the absence of unreacted monomers. Polymers were also characterized through size exclusion chromatography (using an 8-angle static light scattering detector) to determine the molar mass and dispersity of the polymer samples (Table 1). We acknowledge that (co)polymers exhibited variability in their degree of polymerization (molar mass). For this reason, analyses presented below do not take into account the likely, non-negligible influence of molar mass on the properties of the polymers. In doing so, we assume that the polymer structure is the factor determining the polymer properties whereas the molar mass is of secondary importance. Indeed, our recent publication on the antiviral activity of the polymers revealed clear structure-activity correlations with regards to the polymer functionality whereas no clear correlation with the polymer molar mass was observed [21].

2.2. Blood coagulation

Blood pro/anticoagulation is the most known side effect of polyanions upon their systemic administration. Indeed, depending on structure, polyanions may exhibit anticoagulation effect, [49] as is well-known for heparin, [50] a polysaccharide approved by the US FDA specifically for the purpose of blood anticoagulation. Other polyanions such as polyphosphates (nucleic acids) are reported to be pro-coagulants [51]. No interference with blood coagulation is a highly desired safety feature of injectable formulations and identification of coagulation-inert polymers was one of the aims of this study. We investigated activated partial thromboplastin time (aPTT) in presence of the synthesized polyanions. The platelet-depleted plasma from healthy donors was incubated with polyanions at concentrations of 10 or 100 mg/L and the aPTT was measured (Fig. 3). Polysulfonates and PVBzA at 100 mg/L enhanced blood coagulation time to a value over 150 s, similarly to heparin, and this indicates that they are strong blood anti-coagulants. This was also observed with PVPA, which doubled the aPTT value. In contrast, other polyphosphates and polyphosphonates PAPA, PMPA,

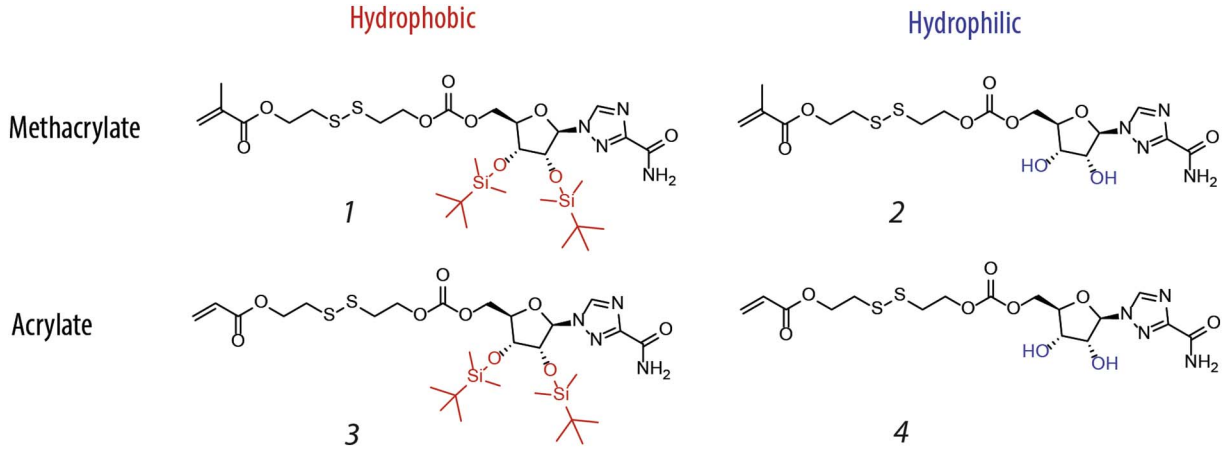

Fig. 2. Four RBV prodrug monomers used for copolymerization with the diverse set of anion containing monomers. For details on monomer syntheses and polymerization conditions, see Experimental Section.

Table 1
Polymerization conditions and macromolecular characteristics of polyanions and macromolecular prodrugs used in this work. For chemical structures and details of synthesis of the RBV containing monomers 1 through 4, see Fig. 1 and Experimental section, respectively. Chain transfer agents were cyanomethyl dodecyl trithiocarbonate (CDTC), (4-Cyano-4-[(dodecylsulfanylthiocarbonyl)sulfanyl]pentanoic acid) (CDPA), cyanomethyl methyl(phenyl)carbamodithioate (CMPD), 2-(dodecylthiocarbonothioylthio)-2-methylpropionic acid (DCMA) or 4-Cyano-4-(phenylcarbonothioylthio)pentanoic acid (CPPA); polymerization initiators were azobisisobutyronitrile (AIBN), 2,2′-Azobis(4-methoxy-2.4-dimethyl valeronitrile) (V-70) or 4,4′-Azobis(4-cyanovaleric acid) (ACVA). M_n: number-average molar mass, SEC-MALS: Size exclusion chromatography with multi-angle light scattering detection, DP: degree of polymerization. Values of dn/dc were calculated from SEC/MALS measurements assuming full mass recovery; DP values for PPAA, PPAA-RBV, and PVBzA (marked with a * symbol) are calculated from M_n (calc). Experimental conditions for anionic homopolymers are taken from Ref. 21.

	RAFT agent	Solvent	RBV monomer	Initiator	°C	Time, h	Conv. A, %	Conv. RBV, %	Mn calc (kDa)	dn/dc	Mn SEC-MALS (kDa)	Đ	DP_{Anion} (GPC)	RBV (%)	RBV, DP
PAA	CDTC	DMF	–	AIBN	60	8	60	–	30.0	0.143	28.3	1.1	393	–	0
PAA-RBV	CDTC	DMF	3	AIBN	60	44	88	95	20.4	0.143	33.8	1.1	413	2	8
PMAA	CDPA	DMF	–	AIBN	60	5.5	77	–	27.3	0.186	57.1	1.2	660	–	0
PMAA-RBV	CDPA	DMF	1	AIBN	60	15	78	92	8.2	0.186	6.7	1.1	64	4	2
PEAA	CDPA	DMF	–	V-70	30	44.5	29	–	5.3	0.165	34.2	1.3	342	–	0
PEAA-RBV	CDPA	DMF	1	V-70	30	69	40	100	17.8	0.186	48.5	1.2	377	5	22
PPAA	CDPA	DMF	–	V-70	30	44.5	55	–	12.6	–	–	–	110*	–	0
PPAA-RBV	CDPA	DMF	1	V-70	30	17.5	36	60	15.4	–	–	–	99*	8	8
PVBzA	CMPD	DMF	–	AIBN	60	4	29	–	9.1	–	–	–	61*	–	0
PAPA	CDPA	Water	–	V-70	30	42	52	–	15.3	0.134	42.2	1.2	235	–	0
PAPA-RBV	CDPA	MeOH/ water	4	V-70	30	68	91	100	27.6	0.180	21.4	1.2	107	4	5
PMPA	CPPA	Water	–	ACVA	70	36	64	–	15.5	0.104	16.6	1.3	86	–	0
PMPA-RBV	CDPA	MeOH/ water	2	ACVA	60	72	100	56	45.0	0.142	99.3	1.4	488	2	10
PAEP	CDPA	MeOH/ water	–	V-70	30	42	99	–	22.2	0.144	21.1	1.1	108	–	0
PAEP-RBV	CDPA	MeOH/ water	4	V-70	30	68	97	100	30.0	0.144	39.4	1.2	174	6	11
PMEP	CDPA	MeOH/ water	–	V-70	30	45	90	–	37.6	0.141	65.6	1.1	314	–	0
PMEP-RBV	CDPA	MeOH/ water	2	V-70	30	64	81	100	45.2	0.104	45.6	1.1	183	7	15
PVPA	CMPD	DMF	–	V-70	30	62	21	–	10.2	0.120	84.6	1.3	783	–	0
PSPA	DCMA	DMF	–	AIBN	60	27	90	–	43.0	0.074	37.6	1.4	162	–	0
PSPA-RBV	DCMA	DMF/water	4	V-70	60	17	97	92	45.8	0.151	64.6	1.1	252	5	13
PAMPS	DCMA	DMF	–	AIBN	60	9	80	–	35.1	0.100	57.2	1.2	276	–	0
PAMPS-RBV	DCMA	MeOH/ DMF/water	3	V-70	60	64	28	43	13.0	0.100	44.9	1.1	185	7	14
PSVBS	DCMA	DMF	–	AIBN	60	26	23	–	9.7	0.148	61.4	1.2	298	–	0
PVSA	CMPD	DMF	–	AIBN	60	18	56	–	12.5	0.938	7	1.1	54	–	0

PAEP and PMEP had minor if any influence on blood coagulation time. Of the carboxylates, PAA and PMAA exhibited a noticeable anti-coagulation effect. In contrast, PEAA and PPAA, two polymers with an enhanced hydrophobicity but decreased anionic character compared to PAA and PMAA (higher pKa) had no effect on blood coagulation time at 10 mg/L. Taken together, results in Fig. 3 reveal that six out of the tested 14 polymers (polyphosphates, polyphosphonates, PEAA and PPAA) appear to have no inhibitory activity with regards to the blood coagulation times.

2.3. Albumin binding

Albumin is the most abundant protein in human plasma. It has numerous physiological functions that include the maintenance of

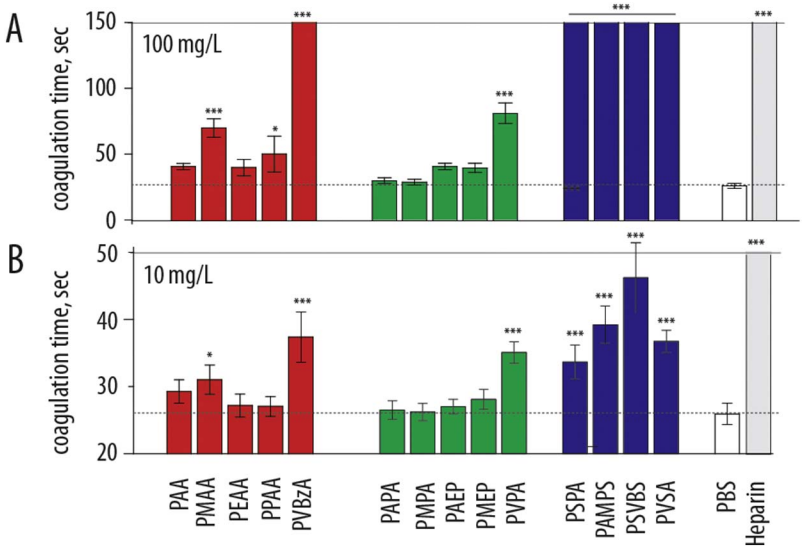

Fig. 3. Blood coagulation time (measured as aPTT) in the presence of polyanions administered at concentration 100 or 10 mg/L. The aPTT was measured for up to 150 s and after that time the sample was considered a strong anticoagulant and its blood coagulation time was set to 150 s. Data for carboxylates are reproduced from Ref. [55]. Dash line indicates the normal blood coagulation time in these experimental conditions and readout. The results are an average of four independent experiments (N = 4; two donors in each experiment) and presented as average ± SD. Statistical significance relative to control was evaluated by a one-way ANOVA with Dunnett's multicomparison post-hoc analysis. *$p \leq 0.05$; **$p \leq 0.01$; ***$p \leq 0.001$.

osmotic pressure and the transport of hydrophobic solutes through the blood. This protein is safe-guarded by the body and physiological mechanisms exist to ensure that albumin is not degraded but retained in the body. As a result, albumin blood residence time reaches a phenomenal value of 3 weeks [52]. Albumin binding is among the most successful methodologies in biomedicine to extend the circulation times of solutes and this has been achieved to a range of drug molecules, from small molecule anticancer drugs [53] to peptide hormones and proteins [54]. Recently, we observed that synthetic polymers (PEAA) can bind albumin and this afforded hepatic deposition of the polymer [55]. Albumin binding for PEAA is not altogether surprising in that this protein is well known to bind hydrophobic solutes and anionic solutes, both features being emphasized in the structure of PEAA. Herein, we aimed to investigate albumin binding for the library of anionic polymers, with and without conjugation of ribavirin. Albumin has several binding sites, most notable of which are the so-called Sudlow I and Sudlow II sites [56,57]. Binding of solutes to these sites can be interrogated using fluorescent probes that exhibit site-specific biding to albumin, specifically dansyl asparagine (Sudlow I) and dansyl sarcosine (Sudlow II) [56]. Fluorescence of these probes is significantly decreased upon displacement from the protein globule, and this presents itself as a facile methodology to quantitate binding of albumin with the polymers. Polymers were mixed with albumin at 5 μM (0.33 g/L) concentration of the protein and 10 molar equivalents of the polymer to albumin. The immediate observation from the results of these experiments (Fig. 4) is that polymers differed significantly in their capacity to interact with albumin via the two nominated sites.

Polyphosphonate polymer PAPA brought about no decrease in the fluorescence of probes indicating no detectable polymer interaction with albumin. PAPA also exhibited no anticoagulation activity (Fig. 3), and together these data suggest that PAPA is a blood-safe carrier for diverse drug delivery applications. Albumin binding for the structurally similar PMPA as well as the phosphate analogues PAEP and PMEP was also not pronounced and at 10-fold mole excess of the polymer to albumin, probe fluorescence decreased by no more than 50%. Polysulfonates also exhibited minor association with albumin and afforded no change in fluorescence for the Sudlow I binding probe and a change in fluorescence for the Sudlow II probe within 50%. Exception to this was the most hydrophobic of these polymers, styrenic PSVBS which showed a 75% probe displacement. In contrast, polycarboxylates exhibited a strong tendency for binding with albumin and exhibited a highly efficacious probe displacement. Binding was not site specific and probes were displaced from both Sudlow I and II sites. In the case of PAA, displacement of probes for both Sudlow I and II sites was near-complete indicating a strong binding. For this polymer, incorporation of RBV abrogated polymer binding to albumin. This illustrates that PAA

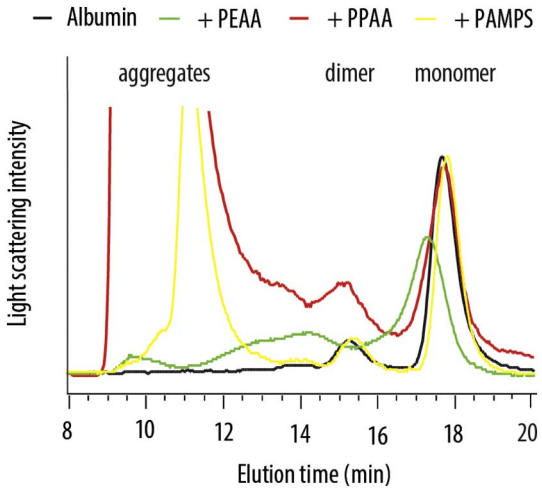

Fig. 5. Size exclusion chromatography elution profiles for equimolar mixtures of albumin with PEAA, PPAA and PAMPS illustrating strong protein aggregation in the presence of PPAA and minor if any interaction of albumin with PAMPS. For PEAA, protein elution profile shifts to shorter elution times indicating an increased hydrodynamic radius of the solute as a result of the polymer-protein interaction.

binding to albumin is structure-programmed and change to this macromolecule such as addition of RBV interferes with albumin binding. PMAA, PEAA and PPAA also exhibited strong probe displacement capacity albeit not as pronounced as PAA. Interestingly, unlike PAA-RBV, PEAA-RBV and PPAA-RBV were strong albumin binders.

Albumin binding was also analyzed by SEC-MALS. This experiment confirmed the difference between the polymers in their capacity to binding albumin and highlighted further changes in the result of the polymer-protein association, Fig. 5. Elution of albumin was hardly altered upon its incubation with PAMPS (polysulfonate) taken at an equimolar concentration to albumin and there was minor protein aggregation in the presence of this polymer. This observation was similar for the protein incubation with PAPA and all polyphosphonates and polyphosphates as well as for PVSA and PSPA. In contrast, for the carboxylates PAA, PMAA, PPAA, PVBZA and the hydrophobic polysulfonate PSVBS, polymer-protein interaction afforded strong aggregation and formation of high molar mass products (MDa). Finally, upon incubation with PEAA, a strong Sudlow I/II probe displacing polymer, elution of albumin was shifted to shorter times indicating increased molar mass of the protein, as would be expected for a polymer-protein adduct, with only minor protein aggregation. PEAA is a unique polymer and albumin binding without noticeable aggregation was not observed

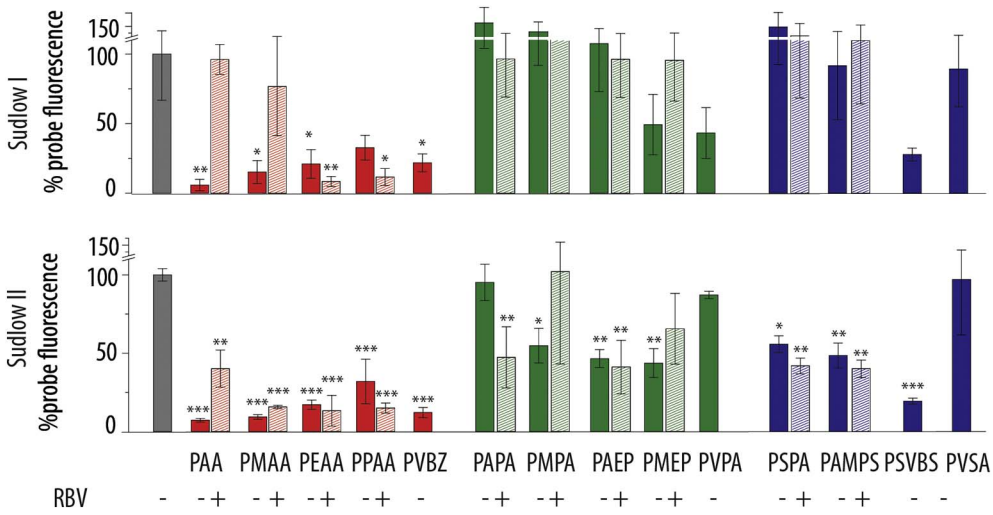

Fig. 4. Polyanions and macromolecular prodrugs exhibit structure-dependent binding to albumin via Sudlow I/II sites. Interaction with albumin was quantified using fluorescent probe displacement assay using dansyl asparagine and dansyl sarcosine as probes for Sudlow I and Sudlow II sites, respectively. Fluorescence intensities of the probe in the presence of polyanions were normalized to that in control experiments. 100% probe fluorescence indicates no probe displacement and 0% probe fluorescence implies quantitative displacement and indicates strong interaction between the polymer and albumin. Results are presented as average of three independent experiments ± SD. Statistical significance compared to the control samples was evaluated via one-way ANOVA with Dunnett's multicomparison post-hoc analysis. *$p \leq 0.05$; **$p \leq 0.01$; ***$p \leq 0.001$.

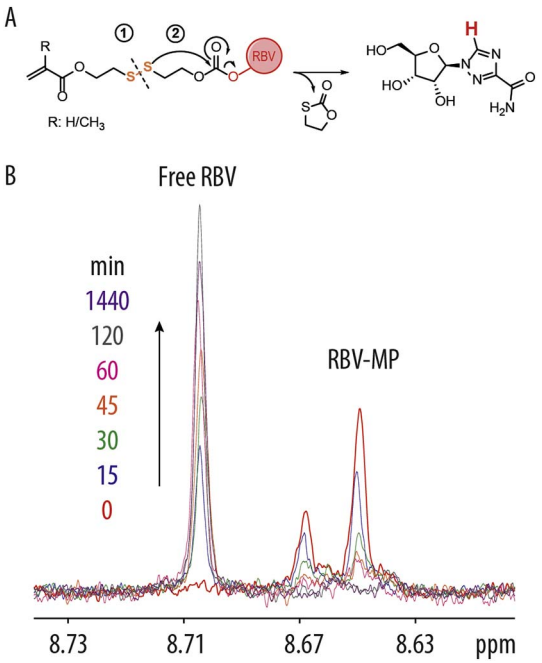

Fig. 6. (A) Schematic illustration of the engineered drug release through the scission of the disulfide bond and the ensuing spontaneous cyclization of the self-immolative linker (B). Illustration of the ^{1}H NMR-based method to monitor and quantify release of RBV from the macromolecular prodrug (PAPA-RBV) through integration of peaks corresponding to bond vs release drug. The proton used for integration is marked in red in panel (A). (For interpretation of the references to colour in this figure legend, the reader is referred to the web version of this article.)

for other polymers studied in this work.

2.4. Drug release kinetics

Next, we examined macromolecular prodrugs with regards to the kinetics of drug release. RBV conjugation was designed such as to be reversed upon the scission of the disulfide linkage, specifically upon cell entry. Intracellular environment is characterized by a relatively high concentration of a thiol containing tripeptide, glutathione (GSH), [58] and this effectively triggers the degradation of disulfide linkages inside the cells [59–61]. Accessibility of the disulfide within the structure of macromolecular prodrugs can vary due to the difference in the size of the side groups functionalities. Polymers may thus exhibit significant differences in the drug release kinetics. We have previously investigated the release of RBV and other drugs conjugated to polymers via the same linkage as used in this study (disulfide trigger paired with a self-immolative linker) via HPLC [43,46,62]. Herein, we established an ^{1}H NMR-based method to quantify the release of RBV as illustrated in Fig. 6 on an example of PAPA-RBV. Macromolecular prodrug was incubated in the presence of GSH. Disulfide reshuffling initiates the spontaneous cyclization of the self-immolative linker with ensuing release of the pristine drug, ribavirin (Fig. 6, A). Chemical shift of the ribavirin protons exhibits a well-defined migration in the ^{1}H NMR spectrum and with time, the signal corresponding to the polymer-bound drug decreases whereas that for the free RBV increases (Fig. 6, B). Integration of the corresponding peaks provides a facile means to quantify RBV bound to the polymer and released from the prodrug. Release of RBV from the macromolecular prodrug was fast and within 1 h, over 75% of the drug was released from the macromolecular carrier (Fig. 7). This kinetics profile is highly advantageous, significantly faster than that reported for the peptide-based linkers between the drug and the carrier, [63] and allows for rapid drug release upon prodrug cell entry. We note that data in Fig. 7 are rather similar to the drug release data collected in our prior studies via HPLC [43,46,62] and this serves to

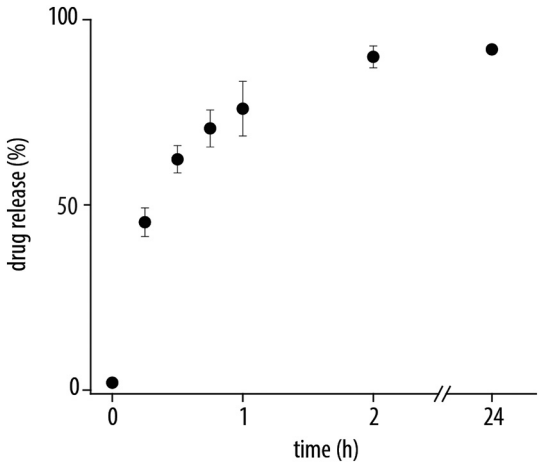

Fig. 7. Kinetics of drug release for PABA-RBV established using the ^{1}H NMR method. Presented results are an average of three independent experiments ± SD.

validate the established herein NMR-based approach to monitor drug release.

^{1}H NMR based method to quantify drug release was applied to the macromolecular prodrugs based on other polyanions as well as a non-ionic carrier, PHPMA, Fig. 8. Within 2 h of observations, all MP exhibited a pronounced release of their payload. A significant finding from this experiment was that hydrophobicity of the polymer chain has a pronounced effect on the kinetics of drug release. In contrast, no such correlation appears to exist with regards to the charge of the polymer (anionic vs charge neutral) or the nature of the negative charge on the polymer. Indeed, structurally similar PHPMA and PMAA as well as PAPA and PAEP released ribavirin quantitatively within 2 h revealing no difference in drug release kinetics. However, relatively small structural change from PMAA to PEAA or from PEAA to PPAA afforded a significant decrease in the drug release. Similarly, a single methyl group variation from PAPA to PMPA afforded a pronounced drop in the amount of RBV released within 2 h. A likely explanation to this phenomenon is the more compact, less hydrated and thus less accessible polymer coil for increasingly hydrophobic polymers which hinder GSH from initiating drug release.

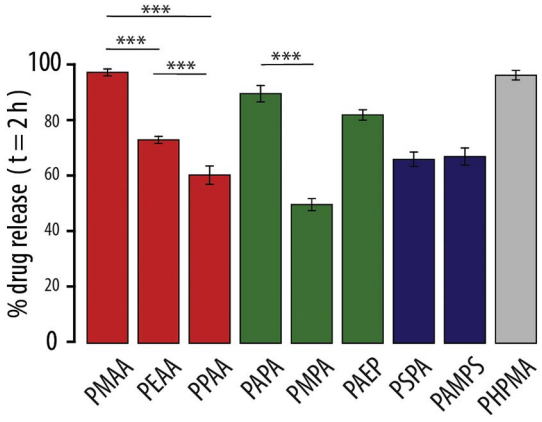

Fig. 8. Drug release analyzed by ^{1}H NMR at 2 h showed a significant decrease in release depending on the hydrophobicity of the carrier in the row of carboxylates (PMAA to PEAA to PPAA), as well as a significantly slower release from the methacrylamide based phosphonate relative to the acrylamide based phosphonate. All data are displayed as mean ± standard deviation from three independent experiments. For comparison a one-way ANOVA (analysis of variance) was performed, followed by a Tukey's post hoc test. ***: P ≤ .001.

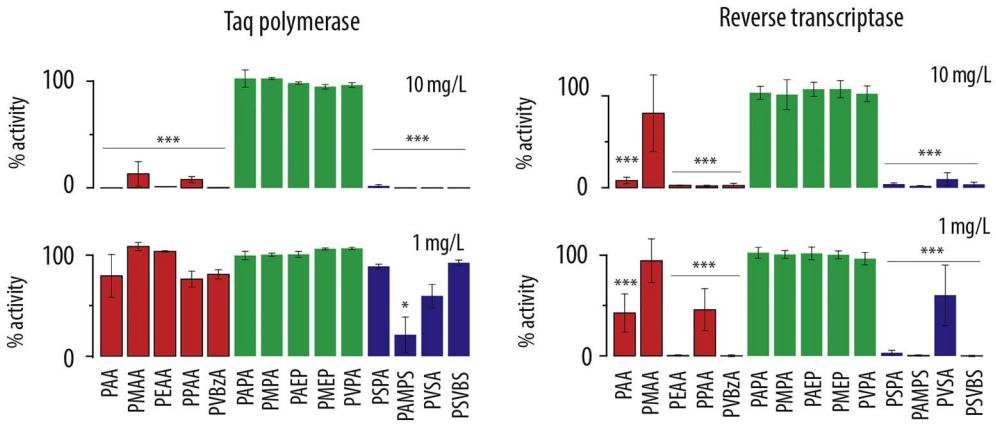

Fig. 9. Activity of the polymerase enzyme in the presence of polyanions (1 or 10 mg/L in the reaction mixture) expressed in % of de novo synthesized nucleic acid relative to the un-inhibited polymerase reaction. Statistical significance compared to control was evaluated via a one-way ANOVA with Dunnett's multicomparison post-hoc analysis. *p ≤ 0.05; **p ≤ 0.01; ***p ≤ 0.001.

2.5. Inhibitory activities on polymerases

Therapeutic and/or side effects elicited by the polyanionic (pro) drugs investigated herein would likely manifest themselves due to the interaction of the polymers with other macromolecules such as proteins. The spectrum of polyanionic endogenous compounds is rather large, and competition [64] for electrostatic interactions with these polymeric partners is highly likely. In the context of antiviral performance of the polymers, we [65] [46] and others [45] have shown that polyanions can act as efficient inhibitors of polymerases. Charge neutral polymers were devoid of such activity [65] pointing to the anionic charge of the polymer (that is, electrostatic interaction with the target) as the origin of the observed phenomenon. Polymers synthesized in this work were analyzed as inhibitors of two types of polymerase enzymes, namely a DNA-dependent DNA polymerase (replicase) and an RNA-dependent DNA polymerase (reverse transcriptase), Fig. 9. Despite being similar in carrying multiple anionic charges, polymers differed markedly in their ability to interfere with the performance of polymerases. Polyphosphates and polyphosphonates were nearly devoid of any inhibitory activity in these assays and regardless of the polymer concentration, polymerases remained uninhibited. Together with the data presented above, e.g. PAPA appears to have unique “stealth-like” properties with no-interference in coagulation assays, albumin binding, and competition for binding with polymerases. In contrast, polycarboxylates and polysulfonates exhibited a dose-dependent polymerase inhibition. A rather surprising finding is that high anionic character alone does not make the polymer a strong inhibitor and in the homologous row of carboxylates, it was PEAA that exhibited the strongest inhibitory activity (complete inhibition of reverse transcriptase activity at 1 mg/L polymer concentration). This observation echoes our recent findings on the apparent unique pairing of negative character and hydrophobicity of the polymer backbone that renders PEAA an efficacious inhibitor of e.g. hepatitis C virus intracellular replication [55] and a lead polymer with broad-spectrum antiviral activity [21]. Similar observation can be made for the negatively charged PVBzA, also characterized by pronounced hydrophobicity of the chain due to the aromatic ring in each repeat unit of the polymer.

2.6. Anti-inflammatory properties

Finally, as a test for activity of the polymers in cell culture, we evaluated polyanions and their counterparts conjugated to RBV as inhibitors of inflammation in stimulated macrophages. Our previous findings revealed that PAA-RBV inhibited the synthesis of an inflammatory marker nitric oxide (NO) in the lipopolysaccharide (LPS)-stimulated macrophages whereby both the polymer and the released drug elicited their individual anti-inflammatory activity [65]. We tested the library of polyanions presented above and quantified inflammatory responses in cells incubated with polymers in a range of concentrations from 0.32 to 200 mg/L. Independently, metabolic activity of the cells (indicative of cell viability) was measured by the Presto Blue assay. These experiments therefore provide information on both, toxicity of the polymers to macrophages in cell culture and anti-inflammatory activity of the polymers.

None of the tested polymers, with or without conjugated ribavirin, exhibited noticeable toxicity at concentrations up to 40 mg/L, Fig. 10. The overall majority of polymers were also devoid of activity with regards to inflammation. However, several polymers comprised notable exceptions and were efficacious inhibitors of inflammation without associated toxicity to the cells. Specifically, among the polyanions, PMAA, PEAA, PVBzA and PSVBS afforded significant decrease in the levels of NO produced by macrophages. An apparent unifying structural feature of these four polymers is that these are the most hydrophobic of the polyanions used in this work. Decreased inflammatory response by PVBzA and PSVBS was observed already at 8 mg/L making these polymers most potent of the tested polyanions. It is also striking that

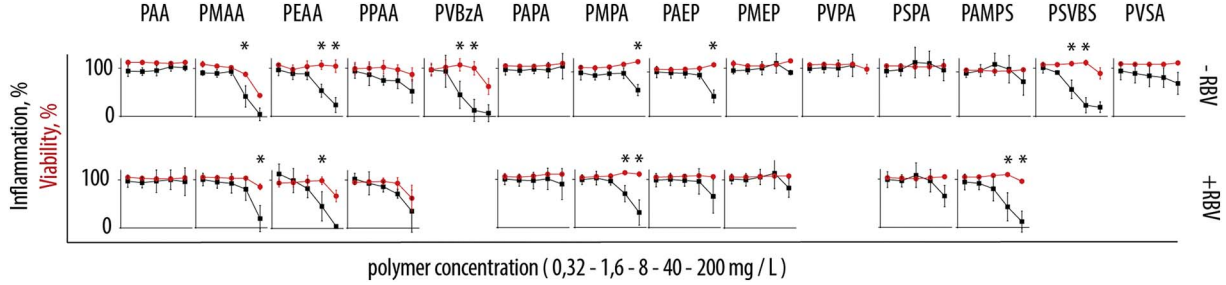

Fig. 10. Concentration-dependent inhibition of inflammation by polyanions and polyanion-RBV conjugates in LPS-stimulated Raw 264.7 macrophages with corresponding cytotoxicity. Raw 264.7 macrophages were stimulated with 1 mg/L LPS and inflammation was measured by quantifying NO via the Griess assay. The concentrations of the polymer which significantly inhibited inflammation without inducing significant toxicity were determined using one-way ANOVA and were marked on the chart with red colour ($p < 0.05$ *). The results are an average of four independent experiments n = 4 ± SD. Statistical significance of results compared to control was evaluated via a one-way ANOVA with Dunnett's multicomparison post-hoc analysis. (For interpretation of the references to colour in this figure legend, the reader is referred to the web version of this article.)

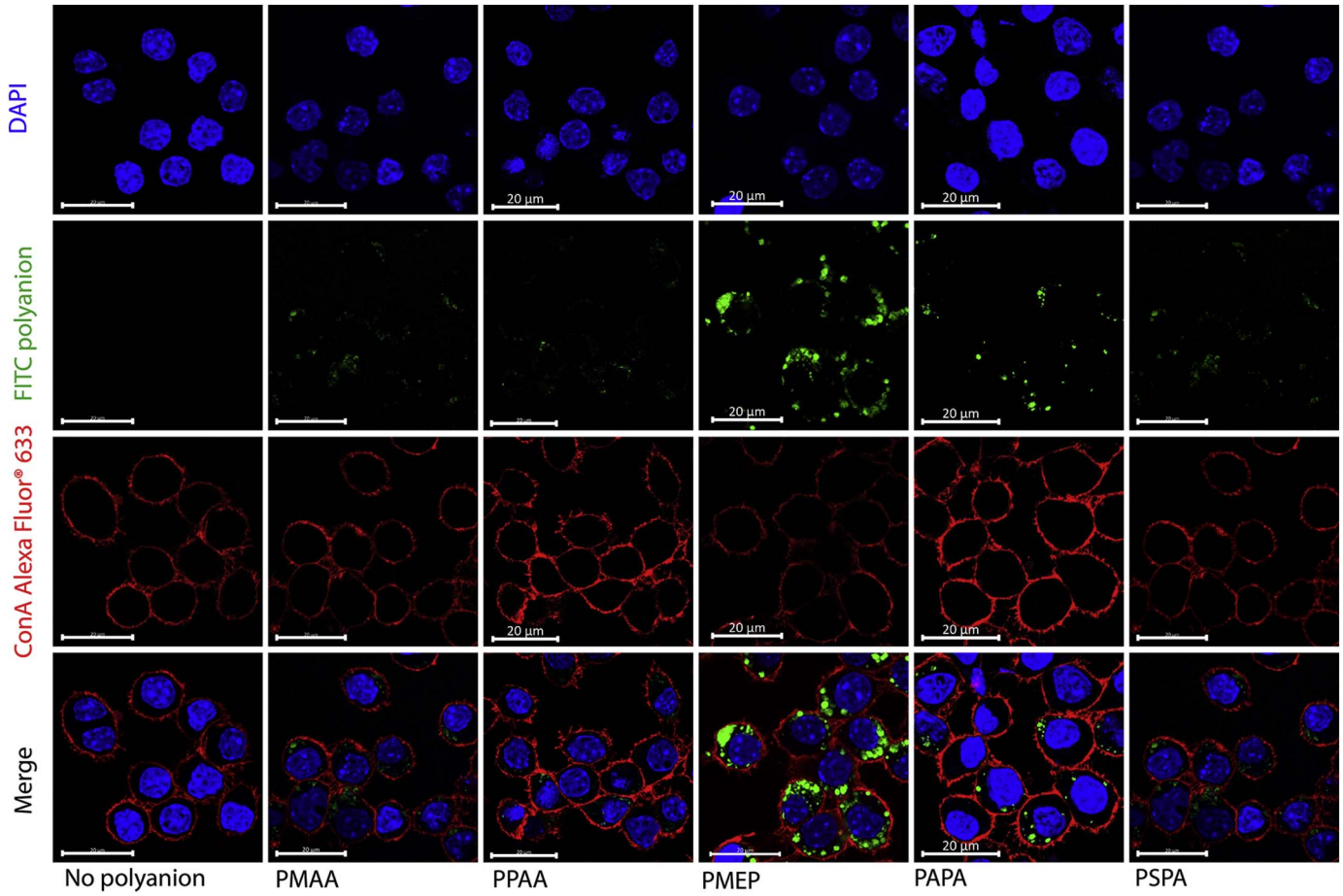

Fig. 11. Confocal microscopy of Raw 264.7 macrophages incubated with 40 mg/L FITC labelled polyanion. Cells are further stained with DAPI and Concanavalin A Alexa Fluor® 633 to visualize cell nuclei and cytoplasmic membrane. First three rows present emission from the three fluorochromes, and the bottom row is a merged image. Scale bar 20 µm.

these two polymers, as well as PEAA, afforded a highly efficacious decrease in the synthesis of NO with a near-complete suppression of inflammation without associated toxicity to the cells. This comes in stark contrast with the RBV based treatment which could only afford ca. 50% reduction in the levels of NO at sub-toxic concentrations of the drug [37]. It is worthy of note that polyanions are typically deemed to have restricted cell entry [66]. However, confocal laser scanning microscopy evaluation of the polymer uptake by macrophages revealed pronounced polymer-associated fluorescence inside the cells (Fig. 11). This was true for all polymers: polycarboxylates, polyphosphates and polyphosphonates, and polysulfonate. Contrary to expectations, cell entry does not appear to be decisive in the observed activity of the polymers.

Macromolecular prodrugs of RBV were synthesized for the (meth) acrylate/(meth)acrylamide type of anionic monomers thus excluding PVBzA, PVPA, PSVBS, and PVSA. Both PMAA and PEAA displayed an inherent, structure-driven effect in the anti-inflammatory assay and in these cases it is therefore not possible to discern the effects elicited by the polymer or the intracellularly released RBV. It is likely that both the polymer and the released drug contribute to the overall anti-inflammatory response in macrophages for PMAA-RBV and PEAA-RBV. Surprising other leads in this assay were macromolecular prodrugs based on PMPA and PAMPS. In both cases, statistical significance of anti-inflammatory effects was observed at concentrations at and above 40 mg/L. This effect was efficacious and had minor if any associated toxicity.

To further probe the mechanism of activity of the polymers in this assay, we investigated potential antagonism of the polyanions with LPS. Indeed, the latter has anionic component to it and competion with polyanions for interaction with the receptor is not inconceivable. Furthermore, prior reports suggested that sulfated polyaromatic suramin can antagonize LPS [67]. To investigate this on the example of PEAA, LPS stimulation of macrophages was performed using increasing concentration of LPS in the presence or absence of a fixed concentration of the polymer (Fig. 12). In this assay, antagonism at the receptor in absence of intracellular effects would manifest itself as a shift in the potency of LPS without a change in efficacy. In turn, intracellular effects in absence of receptor antagonism would mean a decreased efficacy of the inflammatory response with no change in the potency of LPS. Experimental data suggest that both effects are likely observed (Fig. 12) and PEAA exerts its activity through both, receptor antagonism and intracellular effects. Indeed, the polymer affords statistically significant decrease in the inflammation and also a change, albeit a very minor one, in the IC_{50} value for LPS with regards to stimulation of macrophages (0.42 vs 0.24 mg/L in the presence of PEAA).

3. Discussion

Results of this study provide a comprehensive view on polyanions as the backbone for macromolecular broad-spectrum antiviral therapeutics. Together with the results of the screen of these polyanions for inherent antiviral activity, [21] presented data provide a suggestive view on the utility of polyanionic macromolecular prodrugs of ribavirin as antiviral agents (summarized in Table 2).

3.1. Degree of polymerization vs. polymer structure

First, we wish to evaluate the validity of our assumption that

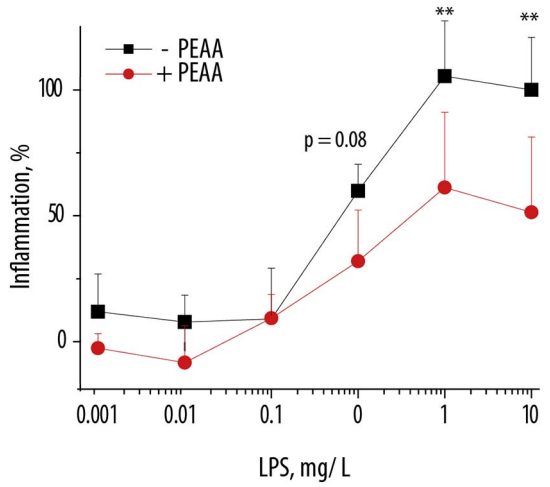

Fig. 12. Competition assay for stimulation of macrophages with LPS in the presence of PEAA. Raw 264.7 macrophages were preincubated with media or with 50 mg/L PEAA and then stimulated with increasing concentrations of LPS. Inflammation was measured by quantifying NO via the Griess assay. The results are an average of three independent experiments n = 3 ± SD. Lower standard error bars were omitted for clarity. The statistical difference in inflammation between PEAA and non-PEAA treated cells was compared using unpaired Student's *t*-test. $p < 0.01$**.

polymer degree of polymerization (molar mass) is of secondary importance compared to the decisive role of the chemistry of the polymer. Indeed, variability between polymers used in this work by the number of repeat units in the chain (Table 2) can mask or skew the observed effects and lead to false negatives or misinterpretation of data. Furthermore, terminal groups arising from the different RAFT agents used in this study to produce the polymers may also considerably change polymer properties [68]. With regards to the latter point, we note that in our hands, macromolecular prodrugs of RBV prior to and after removal of their cleavable end-groups revealed no difference in the anti-inflammatory activity [42]. In this work, to accommodate the synthetic diversity of polymers, we used five different RAFT agents (Table 1) and we see no correlation of polymer activity (Table 2) and the RAFT agent used for the polymer synthesis. Similarly, experimental results presented in this work appear to show no correlation with the polymer molar mass. Blood anti-coagulation effect of the polymers (Fig. 3) shows strong dependence on the nature of the polymer charged functionality (sulfonates > carboxylates > phosphates and phosphonates) but not with M_N (DP). Albumin binding results (probe displacement results, Fig. 4) illustrate that polycarboxylates are strong albumin binders despite the variation of molar mass while phosphate-containing polyanions are weak binders, even the highest molar mass PAPA. Drug release kinetics for macromolecular prodrugs (Fig. 8) shows a statistically significant correlation with the polymer hydrophobicity but not with polymer DP. Polymers most active in RBV delivery were not those characterized by the lowest or the highest DP (in fact, the lowest and the highest DP polymers were not effective in this screen) suggesting that polymer structure, not the number of repeat units in the structure, is decisive in the utility of the polymer as a carrier for the conjugated drug. Without doubt, examples of strong, pronounced effects of molar mass on the biomedical properties of polymers are numerous and importance of this factor should not be overlooked. In our own prior work, with regards to the delivery of RBV, we found that high molar mass restricted the polymer cell entry and in doing so limited the observed therapeutic effects [39,65]. Not disregarding the importance of these observations, the data of this study strongly suggest chemical structure of the polymer is a dominant factor in its properties (at least in the experiments presented in this study) whereas polymer chain length is of secondary importance.

3.2. Structure-activity relationship

The first important conclusion with regards to the activity of polymers is that the lead polymer structures with inherent broad-spectrum antiviral activity (PEAA, PVBZA, PSVBS) [21] appear to also be strong anti-coagulants and strong albumin binders (Figs. 3, 4). In turn, weak anti-coagulants and weak albumin binders are also weak inhibitors of virus infectivity. This conclusion may not be altogether surprising in that both anti-coagulation and antiviral effects are likely due to the interaction between the polymers and a proteinaceous target (for antiviral effects – glycoproteins of the virus capsid). As such, this result implies that polyanionic macromolecular (pro)drugs are not well suited for systemic administration to exert antiviral activity in circulation.

From a different perspective, the three leads with broad-spectrum antiviral activity [21] are also shown in this work to be inhibitory to the activity of polymerases and to possess inherent activity within macrophages, in absence of cytotoxicity. This observation is intriguing in that these three polymers may therefore be inhibitory to viruses both extra- and intracellularly, in part fulfilling the desired combination of antiviral effects. In our view, these polymers become lead candidates for optimization and design of microbicides for non-systemic, localized antiviral treatments. Regretfully, design of ribavirin MP was only considered in this work for (meth)acrylates and (meth)acrylamides; we are currently investigating the synthesis of MP based on PVBzA and PSVBS as a next step in the optimization these antiviral (pro)drugs.

Also worthy of note is the discovery of a family of polyanions that are devoid of any inhibitory activity in the screens we have performed, namely the polyphosphates and polyphosphonates. These polymers appear to have only weak and in most cases minimal interaction with the proteinaceous targets in our assays. Due to this, as well as their high solubilizing power (as is well used in the design of low molar mass prodrugs [53]) and inherent affinity to bone [69], these polymers are highly attractive as carriers for diverse drug delivery applications and specifically for bone targeting.

Table 2
Summary of experimental results of this study and the screen for inherent broad-spectrum antiviral activity (**, taken from Ref. [21]). Results are denoted as "+" if the polymer exhibited the nominated property (being increasingly pronounced on a scale from + to + + +), "−" if the polymer is devoid of this property or effect, and "n/a" if the polymer was not analyzed in this test. Anti-inflammatory activity is denoted '+' if the effect is observed with minimal cytotoxicity of treatment.

	PAA	PMAA	PEAA	PPAA	PVBZA	PVPA	PAPA	PMPA	PAEP	PMEP	PSPA	PSVBS	PAMPS	PVSA
Blood anti-coagulation	+	+	−	−	+ +	+	−	−	−	−	+ +	+ + +	+ + +	+ +
Albumin binding (Sudlow I or II)	+ + +	+ + +	+ + +	+ + +	+ + +	−	−	−	−	+	−	+ +	−	−
Albumin aggregation (in equimolar mixtures)	+ + +	+ + +	−	+ + +	+ + +	−	−	−	−	−	−	+ + +	−	−
Polymerase inhibition	+	+	+ +	+	+ +	−	−	−	−	−	+ +	+	+ +	+ +
Inherent broad spectrum antiviral activity**	−	−	+	−	+ +	−	−	−	−	−	+	+	−/+	+
Cytotoxicity (at 40 mg/L)	−	−	−	−	−	−	−	−	−	−	−	−	−	−
Anti-inflammatory activity for the polymer (at 40 mg/L)	−	+	+	−	+	−	−	−	−	−	−	+	−	−
Anti-inflammatory activity for the MP RBV	−	+	+	−	n/a	n/a	−	+	−	−	−	n/a	+	n/a

4. Experimental section

All chemicals were purchased from Sigma Aldrich and used without further purification unless stated otherwise. Ribavirin was purchased from ApiChemistry.

^{1}H NMR and ^{13}C NMR were recorded with a Bruker BioSpin Gmbh 400 MHz NMR spectrometer. Multiplicities are indicated by abbreviations. s = singlet, bs = broad singlet, d = doublet, t = triplet, p = pentet, m = multiplet. HRMS was recorded on a Bruker Maxis Impact-TOF-MS with electrospray ionization (ESI+). Size-exclusion chromatography (SEC) was performed using a system comprising a LC-20AD Shimadzu HPLC pump, a Shimadzu RID-10A refractive index detector and a Wyatt DAWN HELEOS 8 light scattering detector along with a SPD-M20A PDA detector, equipped with either 1) a HEMA-Bio Linear column with 10 μm particles, a length of 300 mm and an internal diameter of 8 mm from MZ-Analysentechnik in series with a OHpak SB-803 HQ Shodex column with the dimensions 8.0 × 300 mm a particle size of 6 μm or b) Mz-Gel SDplus Linear column with 5 μm particles length of 300 mm and an internal diameter of 8 mm from MZ-Analysentechnik providing an effective molecular weight range of 1000-1.000.000 or c) Superose 6 Increase 10/300 GL from GE healthcare with a pore size of 7 um, a particle size of 8.6 um, an inner diameter of 10 mm and a length of 300 mm providing an effective molecular weight range of 5,000-5,000,000 Da with an exclusion limit > 40,000,000 Da. The solvent used was either a) 0.01 M PBS filtered through a 0.1 μm filter with 300 ppm sodium azide at 1.0 mL/min at 40 °C or b) DMF with 10 mM LiBr, at 1.0 mL/min at 40 °C or c) 0.01 M PBS filtered through a 0.1 μm filter with 300 ppm sodium azide, at 0.75 mL/min at 30 °C. Values of dn/dc used for molar mass calculations were established by Wyatt MALS/Astra software assuming full mass recovery. Plate reader experiments were performed in black 96-well Optiplates on an Enspire 2300 Multilabel Reader (Perkin Elmer®).

4.1. Ribavirin monomer synthesis

4.1.1. Monomer 1

Monomer 1 was synthesized according to the protocol published previously [43].

4.1.2. Monomer 2

Monomer 1 (800 mg, 1.11 mmol, 1 equiv.) was dissolved in dry THF (20 mL) under a N_2 atmosphere. TEA·3HF (0.905 mL, 5.55 mmol, 5 equiv.) was added and the reaction was stirred at room temperature for 24 h. The product was purified by flash column chromatography MeOH/DCM 0:1 to 1:4. Residual triethylamine was removed by dissolving the crude mixture in DCM, washing with NH_4Cl twice, once with water, and once with brine. The organic phase was dried over sodium sulfate, filtered, and concentrated in vacuo yielding the pure product. ^{1}H NMR (400 MHz, DMSO) δ (ppm) 8.82 (s, 1H), 7.88–7.80 (m, 1H), 7.66 (s, 1H), 6.05 (s, 1H), 5.91 (d, J = 2.9 Hz, 1H), 5.73–5.67 (m, 2H), 5.43 (d, J = 5.8 Hz, 1H), 4.42–4.09 (m, 9H), 3.10–2.95 (m, 4H), 1.88 (s, 3H).

4.1.3. 2-((2-hydroxyethyl)disulfaneyl) ethyl acrylate

TEA (8.05 g, 79.55 mmol, 2 equiv.) was added over a cold (0 °C) solution of 2-hydroxyethyl disulfide (12.28 g, 79.64 mmol, 2 equiv.) in DCM (150 mL) under N_2 atmosphere. Acryloyl chloride (3.60 g, 39.77 mmol, 1 equiv.) was added dropwise maintaining the temperature at 0 °C. The reaction mixture was heated slowly to room temperature and stirred for 1 h. The reaction was quenched and washed twice with NH_4Cl and brine. The organic phase was dried over sodium sulfate, filtered, and concentrated in vacuo. The product was purified by flash column chromatography pentane/EtOAc 70:30 to 60:40 yielding the pure product as a light yellow liquid (2.91 g, 35%). ^{1}H NMR (400 MHz, $CDCl_3$) δ (ppm) 6.44 (dd, J = 17.3, 1.3 Hz, 1H), 6.13 (dd, J = 17.3, 10.4 Hz, 1H), 5.87 (dd, J = 10.4, 1.3 Hz, 1H), 4.44 (t, J = 6.7 Hz, 2H), 3.89 (t, J = 5.8 Hz, 3H), 2.97 (t, J = 6.7 Hz, 2H), 2.89 (t, J = 5.7 Hz, 2H), 1.97 (bs, 1H).

4.1.4. Monomer 3

A solution of ((2*R*,3*R*,4*R*,5*R*)-3,4-bis((*tert*-butyldimethylsilyl)oxy)-5-(3-carbamoyl-1H-1,2,4-triazol-1-yl)tetrahydrofuran-2-yl)methyl (4-nitrophenyl) carbonate (4.11 g, 6.25 mmol, 1 equiv.) in dry DCM (120 mL) was added over a cold solution of 2-((2-hydroxyethyl)disulfaneyl)ethyl acrylate (2.69 g, 12.89 mmol, 2 equiv.), DIEA (2.50 g, 19.34 mmol, 3 equiv.) and DMAP (0.157 g, 1.29 mmol, 0.20 equiv.) in dry DCM (350 mL) under N_2 atmosphere. The reaction mixture was stirred at room temperature for 40 h resulting in a conversion of 85%. The reaction was quenched and washed twice with NH_4Cl and brine. The organic phase was dried over magnesium sulfate, filtered, and concentrated in vacuo. The product was purified by flash column chromatography pentane/EtAcO 60:40 to 50:50. Residual *p*-nitrophenol was removed by basic alumina column chromatography EtOAc/MeOH 95:5 yielding the pure product as a colorless solid (1.20 g, 31%). ^{1}H NMR (400 MHz, $CDCl_3$) δ (ppm) 8.40 (s, 1H), 7.01 (s, 1H), 6.43 (dd, J = 17.3. 1.3 Hz, 1H), 6.13 (dd, J = 17.3, 10.4, 1H), 5.86 (dd, J = 10.4, 1.3 Hz, 1H), 5.77 (s, 1H), 5.77 (d, J = 2.8 Hz, 1H), 4.52-4.46 (m, 2H), 4.42 (td, J = 6.6, 2.0 Hz, 4H), 4.30-4.26 (m, 3H), 2.97 (dt, J = 8.8, 6.6 Hz, 4H), 0.90 (s, 9H), 0.88 (s, 9H), 0.07 (s, 9H), 0.02 (s, 3H).

4.1.5. Monomer 4

Monomer 4 was synthesized following the protocol described above with an in situ deprotection performed without purification of the monomer 3. Thus, the crude mixture obtained according to the protocol for the synthesis of Monomer 3 was dissolved in THF (80 mL) under N_2 atmosphere. TEA·3HF (4.45 g, 27.60 mmol) was added and the reaction was stirred for 72 h. The solvent was removed in vacuo and the product was purified by flash column chromatography DCM/MeOH 100:0 to 90:10. Residual TEA was removed by dissolving the product in chloroform and washing twice with NH_4Cl yielding the pure product (0.430 g, 24%). ^{1}H NMR (400 MHz, $CDCl_3$) δ (ppm) 8.81 (s, 1H), 7.85 (s, 1H), 7.65 (s, 1H), 6.35 (dd, J = 17.3. 1.3 Hz, 1H), 6.18 (dd, J = 17.3, 10.4, 1H), 4.96 (dd, J = 10.4, 1.3 Hz, 1H), 5.90 (d, J = 2.8 Hz, 1H), 4.36-4.12 (m, 9H), 3.02 (dt, J = 8.8, 6.6 Hz, 4H).

4.1.6. Polymer syntheses

Experimental details for the syntheses of ethylacrylic acid, propylacrylic acid, 2-methacrylamidoethyl phosphate, 2-acrylamidoethyl phosphate, 2-methacrylamidoethyl phosphonic acid and 2-acrylamidoethyl phosphonic acid were performed according the protocols published previously [21]. Anionic homopolymers were synthesized as previously described in Ref. [21]

4.1.7. Macromolecular prodrugs

Polymer syntheses were performed via RAFT polymerization technique using cyanomethyl dodecyl trithiocarbonate (CDTC), (4-Cyano-4-[(dodecylsulfanylthiocarbonyl)sulfanyl]pentanoic acid) (CDPA), cyanomethyl methyl(phenyl)carbamodithioate (CMPD), 2-(dodecylthiocarbonothioylthio)-2-methylpropionic acid (DCMA) or 4-Cyano-4-(phenylcarbonothioylthio)pentanoic acid (CPPA) as RAFT agents and azobisisobutyronitrile (AIBN), 2,2′-Azobis(4-methoxy-2.4-dimethyl valeronitrile) (V-70) or 4,4′-Azobis(4-cyanovaleric acid) (ACVA) as initiators.

4.1.8. Poly(acrylic acid-co-RBV)

CDTC (2.24 mg, 0.00707 mmol, 1 equiv.) and AIBN (0.166 mg, 0.000707 mmol, 0.1 equiv.) were dissolved in DMF (1.0 mL) and added to a mixture of Monomer 3 (99.77 mg, 0.141 mmol, 20 equiv.) and acrylic acid (0.0916 g, 1.27 mmol, 180 equiv.). Four cycles of freeze-pump-thaw were performed before the ampule was flame sealed under vacuum and the reaction performed at 60 °C for 44 h. The resulting

polymer was purified by precipitation in Et_2O yielding the pure polymer (74 mg). ^{1}H NMR (400 MHz, DMSO-d_6) δ (ppm) 12.28 (bs, 1H), 8.92 (s, 1H), 7.81 (s, 1H), 7.67 (s, 1H), 5.89 (m, 1H), 4.69 (m, 1H) 4.41-4.11 (m, 8H), 2.99 (m, 4H), 2.23-1.39 (m, 3H), 0.94 (s, 9H), 0.82 (s, 9H), 0.10 (s, 6H), 0.02 (s, 3H), -0.22 (s, 3H).

The synthesized polymer (67 mg) was then deprotected using TEA·3HF (0.218 g, 1.35 mmol) in DMF (0.59 mL) at room temperature over 24 h. Resulting polymer was purified by precipitation in dichloromethane yielding the pure product (24 mg). ^{1}H NMR (400 MHz, DMSO-d_6) δ (ppm) 12.19 (bs, 1H) 8.82 (s, 1H), 7.86 (s, 1H), 7.65 (s, 1H), 5.90 (m, 1H) 4.42-4.09 (m, 9H), 2.99 (m, 4H), 1.95-1.10 (m, 3H).

4.1.9. Poly(methacrylic acid-co-RBV)

Methacrylic acid (0.145 mL, 1.72 mmol, 42 equiv.), Monomer 1 (0.357 g, 0.495 mmol, 12 equiv.), AIBN (1.32 mg, 0.00801 mmol, 0.2 equiv.), and CDPA (16.6 mg, 0.0411 mmol, 1 equiv.) were dissolved in DMF (0.2 mL). Five rounds of freeze-pump-thaw were performed before the ampule was flame sealed and the reaction performed at 60 °C for 15 h. The reaction mixture was subsequently diluted with DMF (1.2 mL), TEA·3HF (0.45 mL) was added and the deprotection stirred at room temperature for 20 h. The solution was precipitated into DCM with 5% methanol yielding the pure deprotected product. ^{1}H NMR (400 MHz, DMSO) δ (ppm) 8.82 (s), 7.87 (s), 7.66 (s), 5.91 (m), 4.55–3.99 (m), 2.08–0.34 (m, 5H).

4.1.10. Poly(ethylacrylic acid-co-RBV)

CDPA (9.80 mg, 0.0243 mmol, 1 equiv.) and V-70 (7.12 mg, 0.0231 mmol, 1 equiv.) were dissolved in DMF (0.050 mL) and added to a mixture of Monomer 1 (0.336 g, 0.466 mmol, 19 equiv.) and ethyl acrylic acid (0.480 g, 4.790 mmol, 197 equiv.). Five rounds of freeze-pump-thaw were performed before the ampule was flame sealed and the polymerization was performed at 30 °C for 69 h. The crude was diluted in DMF (3.5 mL) and TEA·3HF (1.29 g, 8.00 mmol) was added. The reaction was monitored by ^{1}H NMR to completion, which was obtained after 24 h of stirring. The purification was performed by precipitation in Et_2O:DCM 1:1 yielding the pure product (221 mg). ^{1}H NMR (400 MHz, DMSO-d_6) δ (ppm) 12.04 (bs, 1H) 8.82 (s, 1H), 7.86 (s, 1H), 7.65 (s, 1H), 5.90 (s, 1H), 4.40-4.11 (m, 9H), 2.99 (m, 4H), 2.16-1.38 (m, 4H), 0.76 (bs, 3H).

4.1.11. Poly(propylacrylic acid-co-RBV)

CDPA (7.39 mg, 0.0183 mmol, 1 equiv.), V-70 (0.00543 g, 0.0176 mmol, 1 equiv.), and Monomer 1 (320 mg, 0.444 mmol, 24 equiv.) were dissolved in DMF (0.1 mL) and added to propylacrylic acid (0.417 g, 3.65 mmol, 200 equiv.) Seven rounds of freeze-pump-thaw were performed before the ampule was flame sealed and the reaction performed at 30 °C for 17.5 h. 1.5 mL DMF and 0.6 mL TEA·3HF was added to the crude and the deprotection stirred for 17 h (monitored by crude ^{1}H NMR). The reaction mixture was precipitated into Et_2O:DCM (1:1) and filtered yielding the pure product (151 mg). ^{1}H NMR (400 MHz, DMSO-d_6) δ (ppm) 8.82 (s), 7.87 (s), 7.66 (s), 5.91 (s), 4.47–4.02 (m), 2.94 (d), 2.09-0.45 (m, 9H).

4.1.12. Poly(3-sulfopropylacrylate-co-RBV)

DCMA (2.26 mg, 0.0062 mmol, 1 equiv.), V-70 (0.382 mg, 0.00124 mmol, 0.2 equiv.), and Monomer 4 (0.052 g, 0.109 mmol, 17.5 equiv.) in DMF (0.2 mL) was added to 3-sulfopropylacrylate (0.245 g, 1.05 mmol, 170 equiv.) dissolved in water (0.2 mL). The polymerization was performed at 60 °C for 17 h. The reaction mixture was diluted with 0.1 M NaHCO3/Na_2CO3 buffer (pH 10.8) and subjected to dialysis in water. A small amount of precipitate was observed in the dialysis tube, and the sample was filtered before lyophilization, obtaining the pure product (100 mg). ^{1}H NMR (400 MHz, D_2O) δ (ppm) 8.63 (s), 5.99 (s), 4.19 (s, 2H), 2.88 (s, 2H), 2.52–1.33 (m, 5H).

4.1.13. Poly(2-acrylamido-2-methylpropane sulfonic acid-co-RBV)

DCMA (2.57 mg, 0.00705 mmol, 1 equiv.) and V-70 (5.1 mg, 0.00165 mmol, 0.2 equiv.), were dissolved in methanol (0.2 mL). Monomer 3 was dissolved in DMF (0.2 mL), AMPS dissolved in water (0.4 mL) was added. Five rounds of freeze-pump-thaw were performed before the ampule was flame sealed and the reaction performed at 60 °C for 64 h. The reaction mixture was diluted with a pH = 10.8 $NaHCO_3$/Na_2CO_3 buffer and purified by dialysis followed by lyophilisation to obtain the pure product (60 mg recovered). ^{1}H NMR (400 MHz, D_2O) δ (ppm) 8.62 (s), 6.08 (s), 3.64–2.35 (m, 3H), 1.41 (s, 9H).

4.1.14. Poly(2-methacrylamidoethyl phosphonic acid-co-RBV)

2-methacrylamidoethyl phosphonic acid (0.115 g, 0.598 mmol, 200 equiv.) was dissolved in acetate buffer (0.3 mL). Monomer 2 (0.0339 g, 0.0688 mmol, 23 equiv.) dissolved in MeOH (0.15 mL) was added together with CDPA (0.00299 mmol, 1 equiv.) and ACVA (0.0015 mmol, 0.5 equiv.) stock solutions. Methanol (0.2 mL) was added giving a slightly unclear solution. Five rounds of freeze-pump-thaw were performed before the ampule was flame sealed and the reaction performed at 60 °C for 72 h. The reaction mixture was diluted with a pH = 10.8 $NaHCO_3$/Na_2CO_3 buffer and purified by dialysis followed by lyophilisation to obtain the pure product (24 mg). ^{1}H NMR (400 MHz, D_2O) δ (ppm) 8.67 (s), 7.83 (s), 3.70 (m), 3.39–2.48 (m, 2H), 2.33–0.09 (m, 7H).

4.1.15. Poly(2-acryalmidoethyl phosphonic acid-co-RBV)

Monomer 4 (0.126 mmol, 24 equiv.), CDPA (0.00214 g, 0.0053 mmol, 1 equiv.), and V-70 (0.00265 mmol, 0.5 equiv.) dissolved in methanol (0.25 mL) was added to 2-acrylamidoethylphosphonic acid (0.0949 g, 0.53 mmol, 100 equiv.) dissolved in water (0.1 mL). Six rounds of freeze pump thaw were performed before the ampule was flame sealed and the reaction was performed at 30 °C for 68 h. The reaction mixture was diluted with a pH = 10.8 $NaHCO_3$/Na_2CO_3 buffer and purified by dialysis, obtaining the pure product upon lyophilisation. ^{1}H NMR (400 MHz, D_2O) δ (ppm) 8.63 (s), 5.98 (s), 4.29 (s), 3.77 (s), 3.24 (s, 2H), 2.87 (m), 1.59 (m, 5H).

4.1.16. Poly(2-methacrylamidoethyl phosphate-co-RBV)

CDPA (0.961 g, 0.0024 mmol, 1 equiv.), V-70 (0.367 g, 0.00119 mmol, 0.5 equiv.), and Monomer 2 (27 mg, 0.0548 mmol, 23 equiv.) were dissolved in methanol (0.3 mL) and added to 2-methacrylamidoethyl phosphate (100 mg, 0.478 mmol, 201 equiv.) dissolved in water (0.1 mL). The mixture was slightly unclear. Five rounds of freeze pump thaw were performed before the ampule was flame sealed and the reaction performed at 30 °C for 64 h. A small amount of precipitate was observed upon reaction, the mixture did not change notably in viscosity. The reaction mixture was diluted with a pH = 10.8 $NaHCO_3$/Na_2CO_3 buffer and purified by dialysis. A second dialysis was performed in 1:1 ethanol/water yielding the pure product which was lyophilized. ^{1}H NMR (400 MHz, D_2O) δ (ppm) 8.77 (s), 7.85 (s), 6.11 (s), 3.90 (s, 2H), 3.37 (s, 2H), 1.81 (m, 2H), 1.38–0.63 (m, 3H).

4.1.17. Poly(2-acrylamidoethyl phosphate-co-RBV)

Monomer 4 (0.129 mmol, 24 equiv.), CDPA (0.0022 g, 0.00545 mmol, 1 equiv.), and V-70 (0.00273 mmol, 0.5 equiv.) dissolved in methanol (0.25 mL) was added to 2-acrylamidoethyl phosphate (0.105 g, 0.538 mmol, 99 equiv.) dissolved in water (0.1 mL). Six rounds of freeze pump thaw were performed before the ampule was flame sealed and the reaction performed at 30 °C for 68 h. The reaction mixture was diluted with a pH = 10.8 $NaHCO_3$/Na_2CO_3 buffer and purified by dialysis. A second dialysis was performed in 1:1 ethanol/water yielding the pure product upon lyophilization. ^{1}H NMR (400 MHz, D_2O) δ (ppm) 8.64 (s), 5.99 (s), 4.28 (s), 3.75 (s, 2H), 3.31 (s, 2H), 2.86 (m), 2.31–0.69 (m, 3H).

4.1.18. Albumin competition assay

The competition assay was performed in 96-well plates, and fluorescence analyzed (excitation wavelength 360 nm, emission wavelength 465 nm) on a plate reader. Polymers were pre-dissolved in minimal amounts of DMSO and then diluted in 0.01 M PBS (pH 7.4). Stock solutions of human serum albumin (HSA) and fluorescent probes (dansyl asparagine/dansyl sarcosine) were prepared in 0.01 M PBS (pH 7.4). The components were mixed and PBS added to obtain a total volume of 100 μL in each well, with the following concentrations: HSA 5 μM, dansyl sarcosine 5 μM or dansyl asparagine 15 μM, and polymer at 50 μM, corresponding to 10 equivalents compared to albumin. Upon mixing the plates were incubated at 37 °C for 1 h to allow the system to equilibrate. The data represents three independent experiments, which each included three technical replicates.

4.1.19. Albumin binding by SEC-MALS analysis

Polymers and albumin (2 g/L) were dissolved in 0.01 M PBS with 300 ppm NaN_3 in equimolar amounts. The samples were incubated for 24 h at room temperature and then directly injected into the SEC-MALS system equipped with a biocolumn and using PBS as an eluent. Results were analyzed using the Wyatt software Astra 6. A sample of albumin with no polymer added was used as reference in order to compare the albumin peak both with regards to the determined molecular weight and the elution times observed.

4.1.20. Drug release kinetics

Ribavirin containing polymers were pre-dissolved in minimal amounts of *d*DMSO (if necessary) and diluted in 0.01 M PBS (pH 7.4) prepared from D_2O. Glutathione (GSH) was also dissolved in 0.01 M PBS (pH 7.4) prepared from D_2O. An aliquot of the polymer solution was mixed with an aliquot of the GSH solution to obtain a 0.4 mL sample containing 2.5 g/L of polymer and 12.5 mM GSH. The sample was incubated for the described time upon which Ellmann's reagent was added in equimolar amounts compared to GSH to quench the reaction. The quenched samples were analyzed by ^{1}H NMR spectroscopy as described in the main text. Time point measurements were repeated at least three times for each polymer.

4.1.21. Anti-inflammatory effect of polyanions in macrophages

Raw 264.7 macrophage cell line (tested negative for mycoplasma) was used to determine the anti-inflammatory activity of polyanions. The cells were seeded on 96-well flat-bottomed plate at initial density of $2 \cdot 10^4$ cells per well in 100 μL of media: high glucose DMEM, stable L-glutamine, without phenol red (Gibco, 21063029) supplemented with 10% FBS and penicillin/streptomycin. Three hours after the cells were seeded, the polymers were added at indicated concentrations in 100 μL of the media and incubated with the cells for 24 h. After 24 h, media was removed and the cells were washed with PBS. Subsequently, the cells were stimulated with LPS (Sigma, L2654) for 24 h. The level of nitric oxide was quantified via Griess assay. Briefly, 50 μL of the cell supernatant was mixed with 50 μL of sulfanilic acid (10 g/L, 5% phosphoric acid). After 5 min of incubation, 50 μL of N-1-napthylethylenediamine dihydrochloride (1 g/L) was added and absorbance (548 nm) was measured using a plate reader (BMG Labtech, Ortenberg, Germany). The level of nitrite was quantified against sodium nitrite standard curve and normalized to the negative control which was LPS-stimulated cells only. Cell viability was measured using PrestoBlue viability reagent (Invitrogen, A13261). Briefly, the cells were incubated with medium containing 10% volume of PrestoBlue reagent. After 1 h of incubation time the fluorescence (570 nm – experimental wavelength, 600 nm – reference wavelength) was measured on the plate reader (BMG Labtech, Ortenberg, Germany). The cell viability was normalized to the viability of the cells incubated with pure media.

4.1.22. Blood coagulation time

The blood obtained from healthy donors was collected into sodium citrate 3.2% tubes. Platelet poor plasma (PPP) was obtained by centrifuging the blood at 3100*g* for 25 min at 20 °C. The polymers were dissolved in PBS buffer containing 5% DMSO. Polymers in the solution were mixed with PPP in volume:volume ratio 1:9 resulting in the final polymers concentration of 10 and 100 mg/L. Prothrombin time was measured using MRX Owren's PT reagent (MediRox, GHI 131-10) and activated partial thromboplastin time was measured using Dade Actin FS (Siemens, B4218-100). All measurements were performed on Sysmex CS-2100i. PBS and PBS with 5% DMSO were used as a negative control. Heparin (Sigma, H3393) was used as a positive control.

4.1.23. Inhibition of DNA-DNA polymerase

To analyze inhibitory effect of polymers on DNA-DNA polymerase activity, quantity PCR (qPCR) reaction was performed using Power SYBR Green PCR Master Mix (Life Technologies) according to the protocol provided by the manufacturer. For one sample 10 μL of Green PCR Master Mix were mixed with forward.

5′-GGTCTCTCTGGTTAGACCAGAT-3′ and reverse primer

5′-CTGCTAGAGATTTTCCACACTG-3′, 0.46 ng of pHXB2-env plasmid (NIBSC, Programme EVA Centre for AIDS Reagents, reference number: ARP206) and a polymer diluted in PBS to a desired concentration. Primers were complementary to LTR upstream element of gag. The program used was 95 °C for 5 min followed by 45 cycles with 95 °C for 12 s, 62 °C for 26 s and during the last cycle, a melting curve was made. A level of inhibition of Taq polymerase was calculated by comparing to a positive control without polymer as 100% of enzyme activity.

4.1.24. Inhibition of RNA-DNA polymerase

Influence of polymers on activity of reverse transcriptase was determined using EnzChek Reverse Transcriptase Assay Kit (Life Technologies). The reaction mixture was prepared according to the protocol provided by the manufacturer. Subsequently polymers diluted in PBS were added at the given concentration, and then 5 U of MuLV Reverse Transcriptase (Life Technologies, Cat. Nr. N8080018). The reaction was performed at 37 °C for 1 h. Nucleic acids were stained with PicoGreen dye and fluorescence was measured on a plate reader (BMG Labtech, Ortenberg, Germany).

4.1.25. Confocal laser scanning microscopy

Cellular uptake of polyanions in macrophages was evaluated by confocal laser scanning microscopy. Coverslips (ThermoFisher Scientific) placed in 24 well plates were coated with 0.01% poly-L-Lysine in water (Sigma-Aldrich) at 37 °C for 2 h, and washed twice with PBS pH 7.4 (Gibco). 10^5 RAW 264.7 cells (mycoplasma negative) were seeded on each coverslip in the 24-well plate in 500 μL media (high glucose DMEM, stable L-glutamine (Gibco) supplemented with 10% FBS and penicillin/streptomycin). 24 h after seeding, media was removed from wells, and 500 μL of 40 mg/L of fluorescently labelled polyanion diluted in media was added to the well. 24 h after addition of polyanions, cells on coverslips were processed for confocal microscopy: coverslips were washed twice with PBS and fixed with 1% paraformaldehyde in PBS for 30 min at RT, followed by washing twice with PBS. Coverslips were stained with 1 μg/mL DAPI in PBS for 10 min, and DAPI was removed by washing twice with PBS. Cell membrane was stained with 50 μg/mL concanavalin A conjugated to Alexa Fluor® 633 (LifeTechnologies) for 30 min at RT. Following this staining step, coverslips were washed twice with PBS and transferred, cells facing down, to a microscopy slide (VWR), and then the cells were submerged in a ProLong™ Diamond Antifade Mountant (ThermoFisher Scientific). Slides were visualised using a ZEISS LSM700 confocal with 63×/1.4 Oil DIC objective, using excitation line 405 nm for DAPI, 488 nm for FITC and 633 nm for Alexa Fluor® 633 with no spectral overlap in collected emission.

Acknowledgements

We wish to acknowledge financial support from the Danish Council for Independent Research, Technology and Production Sciences, Denmark (ANZ; project DFF – 4184-00177).

References

[1] H.D. Marston, G.K. Folkers, D.M. Morens, et al., Emerging viral diseases: confronting threats with new technologies, Sci. Transl. Med. 6 (2014) 253ps210.
[2] R. Lozano, M. Naghavi, K. Foreman, et al., Global and regional mortality from 235 causes of death for 20 age groups in 1990 and 2010: a systematic analysis for the Global Burden of Disease Study, Lancet 380 (2010) 2095–2128.
[3] E. De Clercq, The design of drugs for HIV and HCV, Nat. Rev. Drug Discov. 6 (2007) 1001–1018.
[4] E. De Clercq, G. Li, Approved antiviral drugs over the past 50 years, Clin. Microbiol. Rev. 29 (2016) 695–747.
[5] E. Bekerman, S. Einav, Combating emerging viral threats, Science 348 (2015) 282–283.
[6] B.S. Graham, Advances in Antiviral vaccine development, Immunol. Rev. 255 (2013) 230–242, http://dx.doi.org/10.1111/imr.12098.
[7] C.W. Hendrix, Y.J. Cao, E.J. Fuchs, Topical microbicides to prevent HIV: clinical drug development challenges, Annu. Rev. Pharmacol. Toxicol. 49 (2009) 349–375.
[8] M.M. Lederman, R.E. Offord, O. Hartley, Microbicides and other topical strategies to prevent vaginal transmission of HIV, Nat. Rev. Immunol. 6 (2006) 371–382.
[9] J.-D. Zhu, W. Meng, X.-J. Wang, et al., Broad-spectrum antiviral agents, Front. Microbiol. 6 (2015) 517.
[10] V. Boldescu, M.A.M. Behnam, N. Vasilakis, et al., Broad-spectrum agents for flaviviral infections: dengue, Zika and beyond, Nat. Rev. Drug Discov. 16 (2017) 565–586.
[11] N.B. Finter, S. Chapman, P. Dowd, et al., The use of interferon-alpha in virus infections, Drugs 42 (1991) 749–765.
[12] K.T. Ahmed, A.A. Almashhrawi, J.A. Ibdah, et al., Is the 25-year hepatitis C marathon coming to an end to declare victory? World J. Hepatol. 9 (2017) 921–929.
[13] N.J.C. Snell, Ribavirin - current status of a broad spectrum antiviral agent, Expert. Opin. Pharmacother. 2 (2001) 1317–1324.
[14] E. De Clercq, Antiviral agents active against influenza A viruses, Nat. Rev. Drug Discov. 5 (2006) 1015–1025.
[15] H.-H. Hoffmann, A. Kunz, V.A. Simon, et al., Broad-spectrum antiviral that interferes with de novo pyrimidine biosynthesis, Proc. Natl. Acad. Sci. U. S. A. 108 (2011) 5777–5782.
[16] J.-F. Rossignol, Nitazoxanide: a first-in-class broad-spectrum antiviral agent, Antivir. Res. 110 (2014) 94–103.
[17] H. Zhao, J. Zhou, K. Zhang, et al., A novel peptide with potent and broad-spectrum antiviral activities against multiple respiratory viruses, Sci. Rep. 6 (2016) 22008.
[18] T.P. Sheahan, A.C. Sims, R.L. Graham, et al., Broad-spectrum antiviral GS-5734 inhibits both epidemic and zoonotic coronaviruses, Sci. Transl. Med. 9 (2017).
[19] F. Vigant, N.C. Santos, B. Lee, Broad-spectrum antivirals against viral fusion, Nat. Rev. Microbiol. 13 (2015) 426–437.
[20] A. Vaillant, Nucleic acid polymers: broad spectrum antiviral activity, antiviral mechanisms and optimization for the treatment of hepatitis B and hepatitis D infection, Antivir. Res. 133 (2016) 32–40.
[21] F. Schandock, C.F. Riber, A. Rocker, et al., Macromolecular antiviral agents against Zika, Ebola, SARS, and other pathogenic viruses, Adv. Healthc. Mater. 6 (2017) 1700748.
[22] S.S. Cohen, The isolation and crystallization of plant viruses and other protein macro molecules by means of hydrophilic colloids, J. Biol. Chem. 144 (1942) 353 U329.
[23] H.S. Ginsberg, W.F. Goebel, F.L. Horsfall, Inhibition of mumps virus multiplication by a polysaccharide, Proc. Soc. Exp. Biol. Med. 66 (1947) 99–100.
[24] W.C. Burger, M.A. Stahmann, The combination of lysine polypeptides with tobacco mosaic virus, J. Biol. Chem. 193 (1951) 13–22.
[25] J.R. Rubini, A.F. Rasmussen, M.A. Stahmann, Inhibitory effect of synthetic lysine polypeptides on growth of influenza virus in embryonated eggs, Proc. Soc. Exp. Biol. Med. 76 (1951) 662–665.
[26] A.J. Nahmias, S. Kibrick, Inhibitory effect of heparin on herpes simplex virus, J. Bacteriol. 87 (1964) 1060.
[27] P. Desomer, E. De Clercq, A. Billiau, et al., Antiviral activity of polyacrylic and polymethacrylic acids. I. Mode of action in vitro, J. Virol. 2 (1968) 878.
[28] H. Mitsuya, D.J. Looney, S. Kuno, et al., Dextran sulfate suppression of viruses in the HIV family: inhibition of virion binding to CD4+ cells, Science 240 (1988) 646–649.
[29] A.A.A. Smith, M.B.L. Kryger, B.M. Wohl, et al., Macromolecular (pro) drugs in antiviral research, Polym. Chem. 5 (2014) 6407–6425.
[30] E. De Clercq, Interferon and its inducers—a never-ending story: “old” and “new” data in a new perspective, J. Infect. Dis. 194 (2006) S19–S26.
[31] V. Pirrone, B. Wigdahl, F.C. Krebs, The rise and fall of polyanionic inhibitors of the human immunodeficiency virus type 1, Antivir. Res. 90 (2011) 168–182.
[32] Starpharma, VivaGel® Condom, http://www.starpharma.com/the_vivagel_condom, (2017) , Accessed date: 10 January 2017.
[33] G. Moad, E. Rizzardo, S.H. Thang, Living radical polymerization by the RAFT process – a third update, Aust. J. Chem. 65 (2012) 985–1076.
[34] K. Matyjaszewski, Atom transfer radical polymerization (ATRP): current status and future perspectives, Macromolecules 45 (2012) 4015–4039.
[35] M. Ekblad, B. Adamiak, T. Bergstrom, et al., A highly lipophilic sulfated tetrasaccharide glycoside related to muparfostat (PI-88) exhibits virucidal activity against herpes simplex virus, Antivir. Res. 86 (2010) 196–203.
[36] J. Haldar, D. An, L. Álvarez de Cienfuegos, et al., Polymeric coatings that inactivate both influenza virus and pathogenic bacteria, Proc. Natl. Acad. Sci. U. S. A. 103 (2006) 17667–17671.
[37] M.B.L. Kryger, B.M. Wohl, A.A.A. Smith, et al., Macromolecular prodrugs of ribavirin combat side effects and toxicity with no loss of activity of the drug, ChemComm 49 (2013) 2643–2645.
[38] M.B.L. Kryger, A.A.A. Smith, B.M. Wohl, et al., Macromolecular prodrugs for controlled delivery of ribavirin, Macromol. Biosci. 14 (2014) 173–185.
[39] A.A.A. Smith, K. Zuwala, M.B.L. Kryger, et al., Macromolecular prodrugs of ribavirin: towards a treatment for co-infection with HIV and HCV, Chem. Sci. 6 (2015) 264–269.
[40] T.M. Hinton, K. Zuwala, C. Deffrasnes, et al., Polyanionic macromolecular prodrugs of ribavirin: antiviral agents with a broad Spectrum of activity, Adv. Healthc. Mater. 5 (2016) 534–540.
[41] C.F. Riber, T.M. Hinton, P. Gajda, et al., Macromolecular prodrugs of ribavirin: structure–function correlation as inhibitors of influenza infectivity, Mol. Pharm. 14 (2017) 234–241.
[42] B.M. Wohl, A.A.A. Smith, B.E.B. Jensen, et al., Macromolecular (pro)drugs with concurrent direct activity against the hepatitis C virus and inflammation, J. Control. Release 196 (2014) 197–207.
[43] P. Ruiz-Sanchis, B.M. Wohl, A.A.A. Smith, et al., Highly active macromolecular prodrugs inhibit expression of the hepatitis C virus genome in the host cells, Adv. Healthc. Mater. 4 (2015) 65–68.
[44] P. Vlieghe, T. Clerc, C. Pannecouque, et al., Synthesis of new covalently bound kappa-carrageenan-AZT conjugates with improved anti-HIV activities, J. Med. Chem. 45 (2002) 1275–1283.
[45] M. Witvrouw, V. Fikkert, W. Pluymers, et al., Polyanionic (i.e., polysulfonate) dendrimers can inhibit the replication of human immunodeficiency virus by interfering with both virus adsorption and later steps (reverse transcriptase/integrase) in the virus replicative cycle, Mol. Pharmacol. 58 (2000) 1100–1108.
[46] M. Danial, A.H.F. Andersen, K. Zuwala, et al., Triple activity of lamivudine releasing sulfonated polymers against HIV-1, Mol. Pharm. 13 (2016) 2397–2410.
[47] M. Barz, R. Luxenhofer, R. Zentel, et al., Overcoming the PEG-addiction: well-defined alternatives to PEG, from structure-property relationships to better defined therapeutics, Polym. Chem. 2 (2011) 1900–1918.
[48] C.F. Riber, A.A.A. Smith, A.N. Zelikin, Self-immolative linkers literally bridge disulfide chemistry and the realm of thiol-free drugs, Adv. Healthc. Mater. 4 (2015) 1887–1890.
[49] M. Ciancia, I. Quintana, A.S. Cerezo, Overview of anticoagulant activity of sulfated polysaccharides from seaweeds in relation to their structures, focusing on those of green seaweeds, Curr. Med. Chem. 17 (2010) 2503–2529.
[50] J. Hirsh, S.S. Anand, J.L. Halperin, et al., Guide to anticoagulant therapy: heparin: A statement for healthcare professionals from the American Heart Association, Circulation 103 (2001) 2994–3018.
[51] C. Kannemeier, A. Shibamiya, F. Nakazawa, et al., Extracellular RNA constitutes a natural procoagulant cofactor in blood coagulation, Proc. Natl. Acad. Sci. U. S. A. 104 (2007) 6388–6393.
[52] J.T. Sockolosky, F.C. Szoka, The neonatal Fc receptor, FcRn, as a target for drug delivery and therapy, Adv. Drug Deliv. Rev. 91 (2015) 109–124.
[53] R. Walther, J. Rautio, A.N. Zelikin, Prodrugs in medicinal chemistry and enzyme prodrug therapies, Adv. Drug Deliv. Rev. 118 (2017) 65–77.
[54] A.N. Zelikin, C. Ehrhardt, A.M. Healy, Materials and methods for delivery of biological drugs, Nat. Chem. 8 (2016) 997–1007.
[55] C.F. Riber, A.H.F. Andersen, L.A. Rolskov, et al., Synthetic polymer with a structure-driven hepatic deposition and curative pharmacological activity in hepatic cells, ACS Macro Lett. 6 (2017) 935–940.
[56] P. Caravan, N.J. Cloutier, M.T. Greenfield, et al., The interaction of MS-325 with human serum albumin and its effect on proton relaxation rates, J. Am. Chem. Soc. 124 (2002) 3152–3162.
[57] I. Petitpas, A.A. Bhattacharya, S. Twine, et al., Crystal structure analysis of warfarin binding to human serum albumin - anatomy of drug site I, J. Biol. Chem. 276 (2001) 22804–22809.
[58] V.I. Lushchak, Glutathione homeostasis and functions: potential targets for medical interventions, J. Amino Acids 2012 (2012) 26.
[59] M.H. Lee, Z. Yang, C.W. Lim, et al., Disulfide-cleavage-triggered chemosensors and their biological applications, Chem. Rev. 113 (2013) 5071–5109.
[60] G. Saito, J.A. Swanson, K.D. Lee, Drug delivery strategy utilizing conjugation via reversible disulfide linkages: role and site of cellular reducing activities, Adv. Drug Deliv. Rev. 55 (2003) 199–215.
[61] M. Srinivasarao, P.S. Low, Ligand-targeted drug delivery, Chem. Rev. 117 (2017) 12133–12164.
[62] A. Kock, K. Zuwala, A.A.A. Smith, P. Ruiz-Sanchis, B.M. Wohl, M. Tolstrup, A.N. Zelikin, Disulfide reshuffling triggers the release of a thiol-free anti-HIV agent to make up fast-acting, potent macromolecular prodrugs, Chem. Commun. 50 (2014) 14498–14500.
[63] F. Kratz, I.A. Müller, C. Ryppa, et al., Prodrug strategies in anticancer chemotherapy, ChemMedChem 3 (2008) 20–53.
[64] A.N. Zelikin, E.S. Trukhanova, D. Putnam, et al., Competitive reactions in solutions of poly-L-histidine, calf thymus DNA, and synthetic polyanions: determining the binding constants of polyelectrolytes, J. Am. Chem. Soc. 125 (2003) 13693–13699.
[65] A.A.A. Smith, B.M. Wohl, M.B.L. Kryger, et al., Macromolecular prodrugs of

ribavirin: concerted efforts of the carrier and the drug, Adv. Healthc. Mater. 3 (2014) 1404–1407.
[66] M.B.L. Kryger, S.L. Pedersen, B.M. Wohl, et al., Tools of gene transfer applied to the intracellular delivery of non-nucleic acid polyanionic drugs, ChemComm 52 (2016) 889–891.
[67] G. Strassmann, N. Graber, S.M. Goyert, et al., Inhibition of lipopolysaccharide and Il-1 but not of Tnf-induced activation of human endothelial-cells by suramin, J. Immunol. 153 (1994) 2239–2247.
[68] D. Pissuwan, C. Boyer, K. Gunasekaran, et al., In vitro cytotoxicity of RAFT polymers, Biomacromolecules 11 (2010) 412–420.
[69] S. Monge, B. Canniccioni, A. Graillot, et al., Phosphorus-containing polymers: a great opportunity for the biomedical field, Biomacromolecules 12 (2011) 1973–1982.